A novel SDS-stable dimer of a heterogeneous nuclear ribonucleoprotein at presynaptic terminals of squid neurons

Diego T. P. Lico[a,e], Gabriel S. Lopes[a,e], Janaina Brusco[a,e], José C. Rosa[a], Robert M. Gould[b], Joseph A. DeGiorgis[c,d,e,] and Roy E. Larson,[a,e,*]
[a]Dept. Cellular & Molecular Biology, Faculdade de Medicina de Ribeirão Preto, Universidade de São Paulo, Ribeirão Preto, São Paulo, Brazil 14049-900; [b] Program in Sensory Physiology and Behavior, Marine Biological Laboratory, Woods Hole, MA. 02543; [c]Biology Dept. Providence College, Providence, RI 02918; [d]National Institute of Neurological Disorders and Stroke, NIH, Bethesda, MD 20892; [e]Marine Biological Laboratory, Woods Hole, MA. 02543.
Emails: ditplico@usp.br; gabrielsl@usp.br; janabrusco@gmail.com; jcrosa@fmrp.usp.br; rmgould48@gmail.com; joe_degiorgis@hotmail.com.
*Corresponding author. Tel 55-16-3315-3319; e-mail: relarson@fmrp.usp.br
Short title: RNA-binding proteins in presynaptic terminals

Abstract. The presence of mRNAs in synaptic terminals and their regulated translation are important factors in neuronal communication and plasticity. Heterogeneous nuclear ribonucleoprotein (hnRNP) complexes are involved in the translocation, stability, and subcellular localization of mRNA and the regulation of its translation. Defects in these processes and mutations in components of the hnRNP complexes have been related to the formation of cytoplasmic inclusion bodies and neurodegenerative diseases. Despite much data on mRNA localization and evidence for protein synthesis, as well as the presence of translation machinery, in axons and presynaptic terminals, the identity of RNA-binding proteins involved in RNA transport and function in presynaptic regions is lacking. We previously characterized a strongly basic RNA-binding protein (p65), member of the hnRNP A/B subfamily, in squid presynaptic terminals. Intriguingly, in SDS-PAGE, p65 migrated as a 65 kDa protein, whereas members of the hnRNP A/B family typically have molecular masses ranging from 35 to 42 kDa. In this report we present further biochemical and molecular characterization that shows endogenous p65 to be an SDS-stable dimer composed of ~37 kDa hnRNPA/B-like subunits. We cloned and expressed a recombinant protein corresponding to squid hnRNPA/B-like protein and showed its propensity to aggregate and form SDS-stable dimers *in vitro*. Our data suggest that this unique hnRNPA/B-like protein co-localizes with synaptic vesicle protein 2 and RNA-binding protein ELAV and thus may serve as a link between local mRNA processing and presynaptic function and regulation.
Key words: hnRNP; ribonucleoprotein; presynaptic terminus; synaptosome; Elav; squid.

Abbreviations: BSA, bovine serum albumin; DTT, dithiothreitol; EDTA, ethylenediamine tetraacetate, sodium; EST, expressed sequence tags; hnRNP, heterogeneous nuclear ribonucleoprotein; ORF, open reading frame; PAGE, polyacrylamide gel electrophoresis; PBS, phosphate buffered saline; RNP, ribonucleoprotein; RNP1/ RNP2, core sequences of RNA recognition motifs; SDS, sodium dodecyl sulfate.

Evidence suggests that a subset of mRNAs is selectively located to the extended processes and synaptic connections of neurons, serving as templates for local protein synthesis (Steward and Schuman, 2003; Piper and Holt, 2004). Receptor-regulated mRNA translation occurs in dendrites and post-synaptic terminals and has been implicated in synaptic plasticity (Schuman et al. 2006; Martin and Zukin, 2006; Pfeiffer and Huber, 2006). Evidence has accumulated to confirm the presence of protein synthesis machinery in axons and presynaptic terminals as well (Crispino et al.1993;1997; Martin et al. 1998; Koenig and Giuditta, 1999; Koenig et al. 2000; Bleher and Martin, 2001; Giuditta et al. 2002; Jimenez et al. 2002; Piper and Holt, 2004; Martin, 2004; Atkins et al. 2009), where it may be important for synaptic development (Taylor et al. 2009), injury recovery (Vogelaar et al. 2009), mitochondrial function (Kaplan et al. 2004) and functional plasticity of neuronal transmission (Benech et al. 1999; Gioio et al. 2004; Wang et al. 2009; Willis et al. 2007). It is thought that transcripts and components of the translation machinery have their origin in the neuronal soma and are selectively transported by slow axoplasmic flux to distant synaptic sites, whereas additional factors, including mRNA (Eyman et al. 2007; Sotelo et al. 2014), ribosomes (Court et al.2008; Sotelo et al. 2014) and proteins (Sheller et al. 1995), may be supplied

by surrounding glia and Schwann cells (Koenig and Giuditta, 1999; Twiss and Fainzilber, 2009; Sortelo-Silveira et al. 2006). As mRNAs are transcribed in the nucleus, they are joined with multiple RNA-binding proteins, referred to as heterogeneous nuclear (or messenger) ribonucleoproteins (hnRNPs or mRNPs), to form ribonucleoprotein complexes that control splicing and pre-mRNA processing. These complexes are also believed to function in the translocation out of the nucleus, transport to specific subcellular locations, stability during transport, and priming for translation at distant cytoplasmic locations (Dreyfuss et al. 2002; He and Smith, 2009). Despite much data on mRNA localization and evidence for protein synthesis as well as the presence of translation machinery in the axon and presynaptic terminal, the identity of RNA-binding proteins involved in the function and regulation of local RNA processing at presynaptic regions is lacking.

An important model system that has provided evidence for mRNA translation in the axon and presynaptic terminal is the giant synapse and axon of the squid stellate ganglion as well as the isolated, large presynaptic terminals (synaptosomes) derived from the photoreceptor neurons of squid optic lobes. (Crispino et al. 1993; 1997; Martin et al. 1998; Benech et al.1999; Gioio et al. 2004; Kaplan et al. 2004). We have identified a unique hnRNPA/B-like protein in the presynaptic terminals of squid neurons, which may be involved in local mRNA processing and as such, be an important probe into deciphering presynaptic function and regulation.

Experimental Procedures

Animals and tissue preparation. Optic lobes were dissected from *Doryteuthis pealei* obtained from the Marine Resources Center of the Marine Biological Laboratory in Woods Hole, MA and from *Doryteuthis plei* obtained from the *Centro de Biologia Marinha*-CEBIMar, University of São Paulo, São Sebastião, Brazil. For biochemical procedures optic lobes were quick frozen in liquid nitrogen and stored at -70^{o}C until used. P65 was purified from squid optic lobes by ion exchange chromatography followed by reverse phase chromatography, as described previously (Lico et al. 2010). P37 was obtained in immediately subsequent fractions from the same reverse phase chromatogram. Synaptosomes (isolated terminals from photoreceptor neurons) were prepared from fresh tissue according to Pekkurnaz (Pekkurnaz et al. 2011) with slight modifications. Briefly, each g of optic lobes was homogenized in 5 ml of ice-cold homogenization buffer (HB, 1.0 M sucrose in 20 mM Tris-HCl, pH 7.4) in a Dounce glass-glass homogenizer with a loose-fitting A pestle, by 10-15 gentle strokes. The homogenate was spun at 1,000xg at 4^{o}C for 11 min and then spun at 13,000xg for 45 min. The floating synaptosome layer was carefully freed from the tube wall with a fine needle and decanted into a small Petri dish, gently washed in HB and resuspended in 0.5 ml of HB. A particulate sub-synaptosome fraction (P2) was obtained by resuspending the washed synaptosomes in 3 ml of 20 mM Tris-HCl, pH 7.5 containing Halt Protease Inhibitor Cocktail (Thermo), followed by vigorous homogenization with a Dounce B pestle. This lysed fraction was left on ice for 30 min, before it was centrifuged at 21,000xg for 20 min at 4^{o}C. The pellet (P1) was discarded and the supernatant spun at 150,000xg for 2.5 h. This supernatant was discarded and the high speed pellet (P2) resuspended in 500 μl of 20 mM Tris-HCl pH7.5 containing 0.2 M sucrose, protease inhibitors and 1 mM $MgSO_4$ or 10 mM EDTA where indicated in the figure legend. The P2 fraction was further fractionated on a discontinuous sucrose gradient, containing 0.4, 0.6, 0.8, 1.0 and 1.2 M sucrose steps, by centrifugation in a swinging bucket rotor at 54,000xg for 2 h. Fractions (200 μl) were collected starting from just above the pellet. The pellet was washed and resuspended in 200 μl of Tris buffer. The fractions were analyzed with SDS-PAGE followed by western blotting. In some studies a protein extract from optic lobes was obtained by homogenization of 1 optic lobe (~100 mg) in 1 ml of 50 mM Na-phosphate buffer, pH 7.5, containing 4 M urea, 100 mM NaCl and protease inhibitors, and centrifuged at 40,000 xg for 40 min. at 4°C. The supernatant fraction is referred to as S1 fraction.

Antibodies. The anti-squid RNP2 antibody (α-sqRNP2) was raised in rabbits against the synthetic peptide CLFIGGLSYDTNEDTIKK (BioSynthesis, Lewisville, Texas). The peptide sequence was deduced from the series of b and y ion fragments produced by collision induced dissociation mass spectrometry of tissue-purified p65 and showed high sequence identity and homology to the core sequence of the RNP2 motif in squid. The peptide was conjugated to bovine serum albumin via the NH-terminal cysteine using the maleimide activated BSA conjugation kit (Sigma-Aldrich, St.Louis, MO) following the manufacture´s procedure. Serum was collected from inoculated rabbits and IgG purified on a HiTrap Recombinant Protein A column (GE Health Science, Chalfont St.Giles, UK). This antibody strongly labels 37 kDa polypeptides in brain extracts from squid, chicken, mouse and humans, and therefore should be considered a pan RNP2 antibody. The monoclonal antibodies, mouse anti-synaptic vesicle protein 2 (anti-Sv2) and rat anti-Elav7E8A10 Drosophila protein, were gifts from Dr. Ona Bloom (The Feinstein Institute for Medical Research) and Dr. Ricardo Ramos (University of Sao Paulo)

respectively, both of whom received these antibodies, contributed by K.M.Buckley and G.M.Rubin respectively, from Developmental Studies Hybridoma Bank, created by the NICHD of the NIH and maintained at The University of Iowa, Department of Biology, Iowa City, IA 52242. Secondary antibodies conjugated to peroxidase for Western blotting were obtained from Pierce (Rockford, IL) and conjugated to Alexa 488 and Alexa 564 for immunofluorescence from Molecular Probes (Invitrogen, Carlsbad, CA).

Immunofluorescence. Synaptosomes in suspension were fixed in 1% paraformaldehyde for 6 h at room temperature, adhered to glass microscope slides by incubation for 1 h, washed with phosphate-buffered saline (PBS), and incubated for 30 min in 0.1 M glycine, 0.3% Triton X-100 in PBS, pH7.4; then washed in PBS and blocked in PBS containing 1% BSA, 1% goat serum and 1% Triton X-100 for 1 h at room temperature. The slides were washed with PBS containing 0.3% Triton X-100 and incubated with primary antibody in PBS containing 1% BSA, 1% goat serum, and 0.3% Triton X-100 for 2 h at room temperature. The slides were washed in PBS and incubated with appropriate secondary antibody conjugated to Alexa 488 (Invitrogen) for 1 h and washed again. The slides were mounted in Fluoromount G (Electron Microscopy Sciences, Hatfield, PA) diluted 2:1 in PBS and examined by confocal microscopy. Vibratome sections (30 μm) were prepared from 4% paraformaldehyde-fixed optic lobes embedded in 3% agarose overnight in 10% sucrose in PBS, using a Leica VT1000S vibratome. Slices were blocked in 0.3% fish gelatin and 0.25% Triton X-100 in PBS for 4 h, incubated overnight with primary antibody (1:200) in the same blocking solution at 4^{o}C, followed by secondary antibody conjugated to Alexa 488 for 2 h, transferred to microscope slides, and covered with Vectashield mounting media. After covering with coverslips and removing excess mounting media, the coverslips were mounted on the slides with nail polish and examined by confocal microscopy.

Cloning, sequencing and bacterial expression. Poly(A)+ RNA from *Doryteuthis plei* optic lobes was purified by the guanidine thiocyanate method (Chomczynski and Sacchi, 1987). The hn*RNPA/B-like protein 2* transcript was cloned and amplified from cDNA by PCR using the forward and reverse primers 5´-TCAAAATGCCCGAAAGGTAC-3´ and 5´-GTCTGTAACCGCCCATG-3´, respectively, which were based on contig976 obtained from the *Doryteuthis* databank. The clone was inserted into the pGEM-T vector (Promega). DNA was sequenced using the Big Dye Terminator Cycle Sequencing Ready Reaction (Applied Biosystems) on the ABI 3100 sequence analyzer. In order to express it in bacteria, the ORF was subcloned into the pET-28a vector (Novagen) between the EcoRI and NotI restriction sites using the forward and reverse primers 5´-GGAATTCAAAATGCCCGAAAG GTAC-3´ and 5´-GGCGGCCGC**TTA**TCTGTAACCGCCCATG-3´. The restriction sites are underlined and the complementary stop codon for the C-terminus is in bold. The full construct inserted in this vector contains codons for 6 histidines, a thrombin proteolysis site and 22 irrelevant amino acids in phase with the ORF that begins with the initial methionine. The recombinant protein expressed in BL-21 Star E. coli was induced and expression continued for 3 h at 37^{o}C with agitation at 180 rpm before the protein was purified on a HisTrap FastFlow column (GE Health Science). The *hnRNPA/B-like protein 1* transcript was cloned from *Doryteuthis plei* based on the EST 6207 obtained from the *Doryteuthis* databank and extended by 3´extension (3´RACE, Invitrogen) using the forward and reverse primers 5´-GGAATTCATGCGAGACCCCAATAG-3´ and 5´-GGCCACGCGTCGACTAGTACTTTTTTTTTTTTTTTT-3´, respectively, to extend the sequence to include the 3´stop codon. The full length clone was then obtained for sequencing in the pGEM-T vector by using the forward and reverse primers, 5`-ATGAATTCTATGCCTGAGTCAACCG -3` and 5`-ATGGGCCCTCATCGTCTATAGCCACC - 3`, corresponding to the initial methionine codon up to the 3´stop codon. DNA was sequenced using the Big Dye Terminator Cycle Sequencing Ready Reaction (Applied Biosystems) on the ABI 3100 sequence analyzer.

Oligo(dT) pull-down assay. In order to reduce RNase contamination, centrifuge tubes were treated with 1 M NaOH for 4 h and rinsed extensively with milli-Q water. Other glassware were treated with diethylpyrocarbonate solution (1 ml/l) and autoclaved. OligoTex (dT)-polystyrene-latex (Qiagen, Valencia CA) was washed three times and equilibrated in RNA binding buffer (20 mM TrisHCl, pH7.5 containing 250 mM NaCl, 5 mM EDTA, 0,5% NP-40 and RNAout) (Invitrogen, Life Technologies, Grand Island, NY). The beads were collected by centrifugation at 12-14,000 xg and resuspended in RNA binding buffer to the original volume. The protein sample was diluted 1:1 with 2x RNA binding buffer. 20 μl of OligoTex(dT) resin was added and the mixture incubated for 90 min in the cold room. The resin was collected by centrifugation for 3 min at 12-14,000xg, washed and resuspended in RNA binding buffer to the original volume. Proteins bound to the resin were eluted into SDS-PAGE sample buffer.

Immobilized recombinant hnRNPA/B-like protein 2 pull-down assay. Ni-Sepharose High Performance resin (GE Health Science) was washed and equilibrated in 50 mM phosphate buffer pH 7.5 containing 100 mM NaCl, 5 mM β-mercaptoethanol, and 30 mM imidazol. To avoid using urea, bacteria containing the recombinant construct for the hnRNPA/B-like protein 2 and bacteria containing empty vector (control) were induced overnight at 18^{o}C with agitation at 180 rpm. With this treatment, although most recombinant protein was insoluble, a sufficient amount was soluble in equilibrium buffer without the need for urea. Thus, the supernatants of bacterial lysates were incubated with 50 μl of the prepared resin allowing the recombinant hnRNPA/B-like 2 protein to be coupled via the His-tag-Ni complex. The resin was washed in equilibrium buffer and incubated with protein extracts of optic lobes extracted in phosphate buffer containing 1.5 mM $MgCl_2$ and protease inhibitor cocktail, and centrifuged at 50,000 xg for 30 min at 4^{o}C. Proteins bound to the resin were eluted by SDS-PAGE sample buffer and subjected to SDS-PAGE.

Other methods. SDS-PAGE was performed using 10% minigels (BioRad, Hercules, CA). Urea-PAGE for basic proteins was done on mini gels prepared from 4.5% acrylamide/bisacrylamide, 0.06% ammonium persulfate, 0.1% temed, 0.05% methyl green, in a 80 mM β-alanine and 40 mM acetic acid buffer, pH4.5 (McLellan, 1982), containing 8 M urea. The β-alanine/acetic acid buffer was used as the electrode buffer. Samples were adjusted to 8 M urea in 80 mM β-alanine and 40 mM acetic acid buffer, pH4.5, containing 0.05% methyl green and 10% glycerol. Without boiling, the sample was applied to the gel and the electrophoresis was run at 20 mA toward the anode. Western blotting was done as previously described (Costa et al. 1999). Tryptic peptides from appropriate colloidal Coomassie blue stained bands (Imperial Protein Stain, Pierce Rockford, Il) were analyzed by matrix assisted laser desorption, time-of-flight mass spectrometry (MALDI-TOF/TOF) as previously described (Lico et al., 2010). All mass spectra from MALDI-TOF/TOF were submitted to databank searches using MASCOT against nrNCBI, Swiss-pro and squid ESTs. Multiple sequence alignments were done using the Clustal W algorithm (Higgins and Sharp, 1989). Data mining involved BLAST searches into the NCBI *Doryteuthis* nucleotide database and a squid *Doryteuthis pealei* embryonic transcriptome library from a pooled sequence experiment of stage 16-27 embryos using a 454 sequencing system (Roche), assembled using Newbler software (K.Koenig and J.Gross, University of Texas at Austin, personal communication).

Results

p65 and p37 share immunoreactivity to anti-RNP2 antibody and are endogenous in squid presynaptic terminals.

In a previous study (Lico et al. 2010), we identified and biochemically characterized a highly basic, RNA-binding protein (referred to as p65) that was present in presynaptic terminals of squid optic lobes and stellate ganglia. Based on a sequence deduced from mass spectrometry analysis of tissue-purified p65, we raised a polyclonal antibody in rabbits against the synthetic peptide CKLFIGGLSYDTNEDTIKK , referred to as anti-squid ribonucleoprotein motif 2 (α-sqRNP2) due to its sequence homology to the consensus, RNA-recognition motif, LFIGGL (Maris et al. 2005). This antibody recognized p65 on western blots of optic lobe extracts and isolated presynaptic terminals, as well as the tissue-purified fraction (FIG 1A), thus establishing the correlation between p65 and the peptide antibody. Furthermore, α-sqRNP2 labeled isolated presynaptic endings from the photoreceptor cells in squid optic lobes (synaptosomes) by immunofluorescence (FIG 1B). Confocal microscopy revealed synaptosomes of 5-8 μm in diameter showing intense granular labeling with very little or no background staining in the undefined debris that accompanies this preparation (FIG 1B). The secondary antibody alone did not label these structures (data not shown). Also, comparative staining by immunofluorescence on histological slices of the optic lobe showed similar staining in specific layers within the external plexiform layer by antibodies against synaptic vesicle protein 2 (anti-Sv2), a presynaptic protein, and α-sqRNP2 (FIG 1C). These data and images are similar to those previously obtained with an unrelated antibody that recognized p65 (Lico et al. 2010) and substantiate the localization of p65 within the presynaptic terminals. Surprisingly however, in addition to p65 a 37 kDa polypeptide (p37) was also strongly and consistently labeled by α-sqRNP2 on western blots of these fractions (FIG 1A) suggesting that there was a common epitope being recognized or a strong cross reaction. These immunoreactive species separated into distinct fractions upon reverse phase chromatography (FIG 1A, RPC), indicating distinct molecular properties. These data suggested a very specific relation between p37 and p65 and led us to further investigate the molecular characteristics of and relationship between these proteins.

Peptides derived from mass spectrometric analysis of p65 and p37 correspond to the same hnRNPA/B-like proteins.

Further analysis by mass spectrometry and data mining into squid translated nucleotide databases revealed that, in fact, the fractions containing tissue-purified p65 and p37 contained a mixture of at least two distinct, but highly homologous proteins, encoded by transcripts *hnRNPA/B-like 1* (GenBank accession # RK261459) and *hnRNPA/B-like 2* (GenBank accession # RK261460), respectively (Table 1 and FIG 2). Alignment of the translated, open reading frames (ORFs) of these genes showed 51% identity in primary amino acid sequence between them (FIG 2). A BLASTp search in the NCBI non-redundant protein database clearly indicated that these ORFs correspond to proteins that are members of the phylogenetically conserved, heterogeneous nuclear ribonucleoprotein family, subtype A/B (hnRNPA/B). This subset of RNA-binding proteins is characterized by a linear (amino to carboxyl terminus) organization of structural and functional domains (FIG 2), which include in their amino terminal half two tandem RNA-recognition motifs: RNP2, whose core consensus sequence is LFIGGL, and RNP1, whose core consensus sequence is RGFGFITY (Maris et al. 2005). The A/B subtype is also characterized by glycine-rich sequences in their carboxyl terminal region, which also contains RGG boxes (Krecic & Swanson 1999; He and Smith, 2009), similarly present in these transcripts (FIG 2). The calculated molecular masses for these translated ORFs are 36,317 and 37,621 Da, respectively, which agree with the mobility of p37 in SDS-PAGE (FIG 1A, lane 14). The caveat is that these same two proteins are also encountered in the p65 fraction (Table 1) whose behavior in SDS-PAGE suggests a molecular mass of 65 kDa (FIG 1A, lane 12).

Recombinant hnRNPA/B-like protein 2 is prone to oligomerize.

In order to investigate its molecular properties, we cloned hnRNPA/B-like protein 2 in the pET 28a vector in conjunction with a 6x-histidine tag, expressed it in bacteria and purified it on a Ni^{2+} column. [n.b. Due to the additional histidine residues plus accompanying residues of the vector, the molecular mass of the recombinant protein is 40 kDa.] In order to solubilize and purify hnRNPA/B-like protein 2, the buffers required high concentrations of urea. Notably, purified hnRNPA/B-like protein 2 visually precipitated from solution over time when dialyzed in urea-free buffer. Applied to SDS-PAGE, hnRNPA/B-like protein 2 migrated in accordance with a globular protein of 40 kDa (FIG 3C, lane 1), clearly distinct from p65. We then compared hnRNPA/B-like protein 2 with tissue-purified p65 on non-SDS polyacrylamide gel electrophoresis appropriate for the separation of basic proteins (FIG 3A). Remarkably, hnRNPA/B-like protein 2 showed a graded ladder of molecular species - from a fast mobility, low molecular mass protein, which we assume to be monomeric hnRNPA/B-like protein 2 (40 kDa), to presumably dimeric, trimeric, tetrameric, and higher aggregate species visualized by Coomassie staining and immunoblotting (FIG 3A, lanes 1). This notion of oligomerization is supported by the linearity of the plot of electrophoretic mobility of the Coomassie stained bands versus the logs of the assumed molecular masses of the monomer (40 kDa), dimer (80 kDa), trimer (120 kDa) and tetramer (160 kDa) bands evident in the gel (plot not shown).The mobility of transferrin, a basic protein of 75 kDa (Roberts et al.1966), provided a reference in this gel, which was compatible with the mobility of the presumed 80 kDa dimer of hnRNPA/B-like protein 2. Furthermore, tissue-purified p65 migrated under these non-SDS conditions at ~130 kDa (FIG 3A, lanes 2 and lanes 4), ie. a dimer of its 65 kDa form in SDS-PAGE. When included in the samples, the reducing agent, DTT, collapsed the higher oligomers of recombinant hnRNPA/B-like protein 2 visualized in urea-PAGE down to the monomeric species (FIG 1A, lanes 3) whereas this reagent did not affect the mobility of tissue-purified p65 (FIG1A, lanes 4). Our results suggest that bacterially expressed hnRNPA/B-like protein 2 corresponds to cellular p37 and has an intrinsic propensity to oligomerize that involves disulfide bonding, but may lack appropriate eukaryotic post-translational modifications in order to transform into an SDS-stable dimer and urea-stable tetramer as is characteristic of tissue-purified p65.

Intrinsic factors promote the formation of an SDS-stable dimer of recombinant hnRNPA/B-like protein 2 *in vitro*.

In order to test for post-translational modifications that could induce the specific dimerization of hnRNPA/B-like protein 2 into an SDS-stable conformation, we investigated the effect of optic lobe extracts on the precipitation of hnRNPA/B-like protein 2 at low urea concentrations. When diluted from 4 molar to 1 molar urea in solution at room temperature, hnRNPA/B-like protein 2 visibly precipitated from solution, which was accompanied by a rapid rise in absorption at 600 nm within minutes due to light scattering, reaching a maximum within about an hour (FIG 3B). The falloff in absorption after about 1 h is due to the sedimentation of a visible flocculate that

formed over time. On the other hand, if maintained at 4 M urea no visible precipitate formed and the absorbance was relatively stable over the time lapse of the experiment. The addition of optic lobe extract to the hnRNPA/B-like protein 2 in 1 M urea followed by incubation over the same time period inhibited the precipitation by about 70% during the first hour and prevented the formation of the visible flocculate. The addition of BSA at the same concentration as optic lobe extract did not alter the time course or characteristics of hnRNPA/B-like protein 2 precipitation under these conditions, thus indicating that the effect of the extract was due to an explicit factor in the extract, not a nonspecific protein effect. Notably, when the samples were examined by SDS-PAGE after 16 h of incubation with optic lobe extract, an 80 kDa, SDS-stable, immunoreactive band (dimer) appeared (FIG 3C, lane 3) that was not observed in the sample without extract (FIG 3C, lane 2) nor in the control maintained at 4 M urea (FIG 3C lane 1). Thus, the heavy flocculate did not by itself give rise to SDS-stable dimers. The extract had two remarkable effects on hnRNPA/B-like protein 2 in solution. Firstly, it significantly reduced the degree of precipitation and prevented the flocculation of hnRNPA/B-like protein 2 in 1 M urea, and secondly, it induced the formation of an SDS-resistant dimer. These data support the hypothesis that endogenous factor(s) in the extract produce post translational alterations in hnRNPA/B-like protein 2 that induce its dimerization, giving rise to a stable form equivalent to p65.

Distinct sedimentation properties of p65 and p37 in a sucrose density gradient.

To investigate potential diversity in functional properties between the monomeric and dimeric forms of hnRNPA/B-like protein 2, the high speed pellet fraction (P2) from lysed synaptosomes was applied to a discontinuous sucrose gradient (FIG4A) that is used in mammalian systems to separate 40S RNP particles, that accumulate in the less dense top layers of the gradient, from polyribosomes that accumulate in the more dense bottom layer (Angenstein et al. 2005). Evidence exists for the presence of ribosomes in the large nerve endings of the photoreceptor cells in squid optic lobes (Crispino et al.1997; Martin et al. 1998; Koenig and Giuditta, 1999), the structures that give rise to the synaptosomes that we have used here. On discontinuous sucrose gradients both p65 and p37 mostly accumulated in the 0.2/0.4 M sucrose fractions of the gradient (FIG 4B), consistent with their being part of an RNP 40S complex (Angenstein et al. 2005). In the presence of magnesium ion a significant portion of p65, but not p37, sedimented through the higher density gradient into the pellet fraction (FIG 4B, +Mg). The data is consistent with dimeric hnRNPA/B-like protein 2 having a distinct association with high density RNP complexes, which are suggestive of polyribosomes, since the removal of Mg, which disassembles the eukaryotic polysome, had the effect of reverting the p65 to the less dense region of the gradient (FIG 4B, -Mg).

Tight binding of p65 to oligo(dT)-polystyrene latex beads depends on RNA integrity. Further evidence for distinct properties of the monomer versus the dimer comes from their binding behavior to immobilized oligo(dT), which is used to capture polyA mRNA and associated proteins. Some proteins also directly bind strongly to oligo(dT) in an RNA-independent manner, such as mammalian hnRNPs (Angenstein et al. 2005). We pooled fractions from the 0.2-0.4 M region of the sucrose gradient and incubated them with oligo(dT)- polystyrene latex beads. Both p37 and p65 bound strongly to oligo(dT) and neither were released by eluting the resin in 1 mg/ml heparin, a sulfated proteoglycan that can compete with RNA for electrostatic interactions, or by low ionic strength buffer, which diminishes the interaction between polyA-mRNA and oligo(dT) (data not shown), indicating tight binding to the oligo(dT) resin. Both forms were released by eluting with SDS-PAGE sample buffer (FIG 4C, lane 1). Neither protein bound to oligo(dT) that was preincubated with oligo(dA) (FIG 4C, lane 3) indicating that neither form binds to double stranded oligo(dA/dT) nor to the latex beads non-specifically. Interestingly, treatment of the pooled fraction with RNase before binding to oligo(dT) blocked the capture of dimeric (p65) but not monomeric (p37) hnRNPA/B-like protein 2 (FIG 4C, lane 2); thus, the monomer can bind directly to oligo(dT), whereas the binding of the dimer involves intact RNA.

ELAV-like protein is associated with hnRNPA/B-like protein 2.

Taking advantage of a soluble fraction of the His-tag construction of recombinant hnRNPA/B-like protein 2 (see Experimental Procedures), we immobilized hnRNPA/B-like protein 2 onto Ni^{2+}-Sepharose resin and incubated this with protein extracts of squid optic lobes (FIG 5A) to search for binding partners. Besides recombinant hnRNPA/B-like protein 2 itself, three Coomassie stained bands not detected in the control sample were also captured in the assay (FIG 5A, insert), two of which were immunoreactive to α-sqRNP2 (FIG5A, bands 1, 2) and may be proteolytic or truncated products of hnRNPA/B-like protein 2. The non-immunoreactive band 3 was cut from the gel and analyzed by mass spectrometry, giving the peptides SMFLSIGPIK and ATGYSYGFGFVDYE

that identified it to be an ELAV-like protein (embryonic lethal abnormal vision protein, first described in *Drosophia*), which is an RNA binding protein amply expressed in neurons (Pascale and Govoni, 2012). To verify the association of ELAV protein with endogenous hnRNPA/B-like protein 2, we double-labeled synaptosomes with α-sqRNP2 and an anti-ELAV antibody raised in rats against *Drosophila* Elav. Confocal images showed a high degree of overlap of these two endogenous proteins in granules within the presynaptic structures (FIG 5B).
At least 11 distinct genes in squid encode for members of the hnRNP A/B family of RNA-binding proteins. Besides the NCBI *Doryteuthis* database, which mostly contains expressed sequence tags from the stellate ganglia of the north Atlantic squid (DeGiorgis et al, 2011), we also searched a *Doryteuthis* whole embryonic transcriptome library (K.Koenig and J.Gross, University of Texas at Austin, personal communication). We found 11 distinct ORFs with primary and domain structure homologous to the hnRNPA/B subtype (FIG 6). At least 6 of these appear to be complete sequences, each having a potential initial methionine codon that conforms to a Kozak-like rule (Kozak 1989) for initiation of translation (AxxAUGC/G,) , positioned closely upstream from the consensus RNP2 motif, and a conserved C-terminal triplet Y/sR/sR immediately before the stop codon. The N-terminal half of these molecules are highly conserved, with almost no gaps needed for alignment. The exception is a large gap introduced in 10 sequences to accommodate an insertion in isotig15030, the largest and most variant sequence included here. The C-terminal half is the most varied region for primary sequence identity, yet 8 sequences have RGG boxes and 9 are glycine-rich. Although the transcriptome for *Doryteuthis* is not complete and thus this analysis must be considered partial, we can perceive the complexity of this family and the numerous possibilities for selective interactions in RNP complex formation and in regulation of RNA processing.

Discussion

In this report we have presented biochemical and molecular evidence showing that an endogenous, strongly-basic 65 kDa protein (p65) localized in squid presynaptic terminals is an SDS-stable dimer composed of ~37 kDa hnRNPA/B-like subunits. The evidence for this is i) a peptide-derived, polyclonal antibody immunoreactive to p65 also recognized a 37 kDa protein (p37) in subcellular fractions by western blotting; ii) mass spectrometric analysis of tissue-purified p65 and p37, and BLAST searches into the NCBI *Doryteuthis* nucleotide database, identified the same two, highly homologous, hnRNPA/B-like proteins in both the p65 and p37 fractions; iii) bacterially expressed and purified recombinant hnRNPA/B-like protein 2 showed propensity to oligomerize in acidic buffer as analyzed by urea-PAGE, which included the formation of dimers that however were not stable as such in SDS; iv) incubation of the recombinant hnRNPA/B-like protein 2 with small amounts of optic lobe extract produced an SDS-resistant dimer visualized on SDS-PAGE, which suggests that endogenous factor(s) can induce post-translational modifications in hnRNPA/B-like protein 2 that promote the formation of the SDS-stable dimer. The precise molecular definition of what composes the p65 dimer is still ambiguous. The data support the hypothesis that endogenous p65, a highly basic protein as determined by two-dimensional electrophoresis and ion exchange chromatography (Lico et al, 2010), is a homodimer of hnRNPA/B-like protein 2 (isoelectric point, pI 8.9), but not a homodimer of hnRNPA/B-like protein 1 (pI 7.1). However, we have not excluded the possibility that p65 is a heterodimer containing both hnRNPA/B-like proteins 1 and 2 (combined pI is 8.6). Also, the large number of highly homologous hnRNPs in squid allows for the possibility that many different combinations of hnRNPA/B-like protein 2 with another RNP could exist and thus advocates caution on defining the heterodimer. Further investigation is underway to also characterize hnRNPA/B-like protein 1 and determine its possible role as a binding partner.

The hnRNPA/B proteins compose an abundant and structurally conserved family of RNA-binding proteins that form core elements in ribonucleoprotein complexes involved in packaging of nascent mRNAs into granules that can shuttle out of the nucleus and locate to distant cytoplasmic compartments, such as the synapse, where they may play roles in local RNA processing, RNA stability, and regulation of translation (Sossin and DesGrosillers, 2006; Sotelo-Silveira et al., 2006; Akins et al., 2009). In part, these processes require reversible and regulatable protein-protein and protein-RNA aggregation of key components in the granules to induce a shift from repressive to active translational function. Both monomeric and dimeric forms of hnRNPA/B-like protein 2 are endogenous in presynaptic terminals, where they show differential association with particles of distinct densities (FIG 4B). Also, their difference in dependence on RNA for binding to oligo(dT) resin (FIG 4C) suggests that dimerization could act as a switch that determines subcellular associations and function, perhaps masking and unmasking mRNA to allow local translation under appropriate conditions. *In vitro* studies

demonstrated that pure recombinant hnRNPA/B-like protein 2 was prone to oligomerize and that catalytic amounts of optic lobe extract could induce it to form SDS-stable dimers, indicating that dimerization could be regulated by intrinsic factors. Furthermore, the association with ELAV, a key RNA-binding protein in RNA granules that binds to adenine-uridine rich elements, and their co-localization in granules in presynaptic terminals further implicate squid hnRNPA/B-like protein 2 in local RNA processing and/or regulation of its translation.

Dynamic protein-protein and RNA-protein binding is part of the normal physiological functions for RNP complexes. So, the propensity to aggregate reversibly is an important property for components of RNA granules. However, this important property may have the dire consequence of facilitating uncontrolled aggregation, particularly when genetic risk factors are present. The formation of insoluble, SDS-resistent , fibrillar aggregates in cytoplasmic inclusion bodies is a hallmark feature of several neurodegenerative diseases. This includes the hnRNPA/B proteins, which are prone to form these structures, especially when exacerbated by disease mutations (Kim et al. 2013). Furthermore, hnRNPA2/B1 and hnRNP A1 are capable of binding with TAR DNA binding protein-43 (TDP-43) (Buratti et al, 2005), an important hnRNP identified in inclusion bodies of patients with amyotrophic lateral sclerosis and frontotemperal lobar degeneration (Winton et al, 2008). Note that TDP-43 is composed of an N-terminal region with two RNA recognition motifs and a glycine-rich carboxy terminal domain similar to the squid hnRNPA/B-like proteins, although it does not share primary sequence homology with any that we have identified. A further example of pathological aggregation is the sequestering of hnRNPA2 in RNA foci in the fragil-X-associated ataxia syndrome (Iwahashi et al, 2006). It is not clear exactly what the role of inclusion bodies is in the disease process, although one attractive idea is that inclusion bodies capture RNA-binding proteins by ungoverned aggregation, disrupting their normal function and thus deregulating local RNA processing and translation at the synapse.

In summary, p65 is an interesting subject for further investigation in the context of having a high degree of structural homology to the hnRNPA/B subfamily of RNA-binding proteins, and existing in presynaptic, subcellular fractions of squid neurons uniquely in two stable forms. An understanding of the molecular and biochemical mechanisms involved in the stability of the dimeric form, and the regulation and function of the transition between monomeric and dimeric forms may bring insight into not only the role of site-specific RNA processing at the synapse but also shed light on inclusion body formation in neuropathologies.

Table 1. Identification of squid genes containing peptides obtained by mass spectrometry analysis of tissue-purified p65 and p37. Peptide sequences were derived from mass spectroscopy analysis applied to the tryptic digestion of tissue-purified p65 and p37 cut from colloidal Coomassie-stained SDS-PAGE gels after reverse-phase chromatography (see FIG 1A, RPC lanes 12 and 14, respectively). These sequences were used to probe the NCBI nucleotide database with the tBLASTn program choosing *Doryteuthis* as the target organism. ESTs containing open reading frames having exact correspondence to the mass spectrometry peptides were found. Based on these ESTs, two hnRNPA/B-like genes were cloned and sequenced from *Doryteuthis plei* (GenBank accession numbers KR261459 and KR261460, respectively).

protein	ion mass	Derived amino acid sequence	GenBank accession n^{o}
p65	1448.61	DDNDDPQAEKFR	KR261460
p65	1673.61	GGGGGGGGGG	KR261460
p65	1106.47	EDTSEEEIR	KR261459
p65/p37	931.43	GFGFITYK	KR261459 KR261460
p37	1812.91	LFIGGLNYDTTEETIK	KR261460
p37	1695.79	AAEMLDDAQTNRPHK	KR261460
p37	1766.81	MFVGGLKDDTAEDDVR	KR261460
p37	860.54	LFVGGIK	KR261459
p37	1348.69	GKIESIDMITDK	KR261459
p37	1799.87	LFIGGLNYTTNEEAMK	KR261459
p37	2117.00	GFGFITYKTEEQVDEAQR	KR261459

Figure legends

Fig 1. p65 and p37 are present in extracts and subcellular fractions of squid optic lobes. (A) Western blots after SDS-PAGE of subcellular fractions from squid optic lobes were probed with α-sqRNP2 and developed by chemiluminescence. As described in Experimental Proceedures: H, homogenate; S, the supernatant underlying the synaptosome floating layer; Syn, the synaptosomal fraction; P2, the high-spin pellet from lysed synaptosomes; lanes 12, 13, and 14 are fractions from reverse phase chromatography (RPC) containing the peak of p65 (lane 12) and immediately following fractions (lanes 13 and 14) containing p37 (see Lico et al. 2010 supplementary figures at http://dx.doi.org/10.1016/j.neuroscience.2009. 12.005 for chromatography profiles) . The positions of the immunoreactive bands corresponding to p65 and p37 are indicated to the right of the figure; positions of molecular mass standards are indicated to the left. **(B)** Confocal image of synaptosomes immunolabeled with α-sqRNP2 as primary antibody and Alexa 488 conjugated to secondary antibodies is illustrated in the left hand panel. The right hand panel shows the DIC image of these synaptosomes. Controls of synaptosomes probed with only the secondary antibody were not labeled (data not shown). **(C)** Transversal vibratome sections of squid optic lobes were stained with DAPI to label nuclei (rendered in red) and probed with anti-synaptic vesicle protein 2 (α-Sv2) (green, left panel) or with α-sqRNP2 (green, right panel). The arrows indicate the immunopositive layers in the outer plexiform layer common to both antibodies. The asterisk indicates a layer labeled by α-Sv2 but not clearly detected by α-sqRNP2. The morphological layers described by Haghighat et al. (1984) are indicated to the right of the images: ON, outer nuclear layer; OPX, outer plexiform layer; IN, inner nuclear layer; IPX, inner plexiform layer; and MN, mononuclear layer.

Figure 2. Alignment of translated ORFs corresponding to *hnRNPA/B-like proteins 1* and *2*.The ClustalW program was used to align the predicted amino acid sequences of *hnRNPA/B-like proteins 1*(prot 1) and *2* (prot 2). Amino acid identity is indicated by an underlying asterisk and chemical homology by double dots. The boxed areas indicate the core sequences for the RNA-recognition motifs RNP1 and RNP2 as indicated. RGG triplets making up the RGG boxes are underlined. Peptide sequences derived from mass spectrometry analysis of tissue-purified p65 and p37 are in bold print.

Figure 3. The recombinant protein, hnRNPA/B-like protein 2, shows propensity to form urea- and SDS-stable oligomers. (A) The recombinant protein hnRNPA/B-like protein 2 (rp2), expressed in bacteria and purified on a Ni^{2+}- affinity column, was compared to tissue-purified p65 by polyacrylamide gel electrophoresis in the presence of 8M urea in a β-alanine/acetate buffer, pH4.5 (UREA-PAGE), appropriate for the separation of basic proteins. Gels were stained by colloidal Coomassie Blue (CCB). The same samples were applied on equivalent gels and blotted to a nitrocellulose membrane for immunoprobing with α-sqRNP2 (WB). Lane TF, transferrin (10 μg), applied as a 75 kDa, basic-protein indicator (the unidentified lower mobility band (asterisk) seen in the gel appears with overloaded sample application). Lanes 1, recombinant hnRNPA/B-like protein 2 (10 μg). Lanes 2, tissue-purified p65 (5 μg). Lanes 3, recombinant hnRNPA/B-like protein 2 plus 175 mM DTT. Lanes 4, p65 plus 175 mM DTT. Indicated in lanes 1 by i, ii, and iii are the presumed dimeric, trimeric and

tetrameric forms, respectively, of the recombinant hnRNPA/B-like protein 2 (rp2). **(B)** Precipitation of recombinant hnRNPA/B-like protein 2 from 1M urea was followed at the indicated times by light scattering at 600 nm over a 16 h period at room temperature. Cuvets containing 62 μg/ml recombinant hnRNPA/B-like protein 2 in 4 M urea (—▲—), in 1 M urea (—●—), in 1 M urea and 110 μg/ml BSA (—■—), in 1 M urea and 110 μg/ml optic lobe extract (—□—) or in 1 M urea and 220 μg/ml optic lobe extract (—○—) were incubated at room temperature. **(C)** Western blot probed with α-sqRNP2 of samples incubated for 16 h. Lane 1, recombinant hnRNPA/B-like protein 2 in 4 M urea. Lane 2, recombinant hnRNPA/B-like protein 2 in 1 M urea. Lane 3, recombinant hnRNPA/B-like protein 2 in 1 M urea and 110 μg/ml optic lobe extract. Lane 4, 110 μg/ml optic lobe extract alone. The SDS-stable dimer of recombinant hnRNPA/B-like protein 2 is indicated (dimer); rp2 indicates the monomeric form.

Figure 4. In the presence of magnesium ions, p65 cosediments on a discontinuous sucrose gradient with the high density fraction from lysed synaptosomes. The high speed pellet from lysed synaptosomes (P2) was resuspended in 20 mM Tris-HCl, pH7.5, containing 0.2 M sucrose, a cocktail of protease inhibitors and in addition where indicated, 1 mM $MgSO_4$ (+Mg) or 10 mM EDTA (-Mg). This was then applied to a 0.4 to1.2 M sucrose discontinuous gradient and centrifuged at 54,000 xg for 2 h at 4°C. Ten 0.3 ml fractions (1-10) and the gradient pellet (P) were collected and analyzed by SDS-PAGE and western blotting with α-sqRNP2. **(A)** Coomassie stained gel (CCB) after SDS-PAGE of the gradient fractions. Mobilities of molecular mass markers (kDa) are shown in lane M and approximate sucrose concentrations in the fractions are indicated above. **(B)** The upper panel shows the western blot of equivalent fractions from a gradient in the presence of Mg (+Mg) and lower panel with EDTA added to remove Mg (-Mg). Mobility positions of p65 and p37 are indicated to the right of the figure. **(C)** Western blot of pooled fractions from the 0.2 and 0.4 M regions of sucrose gradients incubated with Oligotex (dT) polystyrene-latex beads as described in Experimental Procedures. Both p65 and p37 bound tightly to the beads and were eluted in SDS-PAGE sample buffer (lane 1). Treatment of the pooled fraction with RNase A (10 μg/ml) for 30 min before incubation with the resin blocked the binding of p65 but not p37 (lane 2). Incubation of oligo(dA) with the Oligotex(dT) beads before addition of the pooled fraction blocked the binding of both p65 and p37 (lane 3).

Figure 5. Pull-down assays indicate association of p65 and p37 with RNP granule complexes. (A) The pull-down fraction was obtained by binding His-tagged recombinant hnRNPA/B-like protein 2 to Ni^{2+}- Sepharose and incubating the complex for 2 h at 4°C with extracts of squid optic lobes as described in Experimental Procedures. The control (Ct) was an equivalent reaction lacking only recombinant hnRNPA/B-like protein 2. The pull-down fraction (PD) was analyzed by SDS-PAGE (CCB) and western blotting (WB). Besides recombinant hnRNPA/B-like protein 2 (insert, rp2), three Coomassie-stained bands (insert, bands1,2,3) not detected in the control were seen. Bands 1 and 2 were immunoreactive to α-sqRNP2 by western blotting and may represent breakdown products or truncated expression of recombinant hnRNPA/B-like protein 2. The faster migrating, non-immunoreactive band 3 was analyzed by mass spectrometry and identified as the neuron specific, RNA-binding, nELAV-like protein (Pascale and Goconi, 2012). **(B)** Confocal images of two representative synaptosomes that were double immunolabeled with α-sqRNP2 polyclonal antibody (green) and anti-ELAV monoclonal antibody (α-Elav, red) are shown. The merged images show yellow where overlap occurs. The far right hand panels show the DIC images. Controls of synaptosomes probed with only the secondary antibodies were not labeled (data not shown).

Figure 6. Sequence alignment of squid proteins having hnRNPA/B-like primary structure. The translated nucleotide database of *Doryteuthis* from NCBI (*contigs*) and the squid embryo RNAseq database (*isotigs*) were data mined for ORFs having primary sequences consistent with the domain structure of the hnRNP A/B subtype of RNA-binding proteins, ie. tandem repeats of the RNP2/RNP1 motifs. **(A)** The highly conserved N-terminal halves of 11 ORFs were aligned using CLUSTAL W 2.1.The cores of the RNA recognition motifs are indicated by underlined bold type. Identical and highly homologous regions are shaded. Potential initial methionines at the N-terminus that conform to a Kozak-like rule (Kozak, 1989) for initiation of translation (AxxAUGC/G) are indicated in shaded bold. **(B)** The sequences in the C-terminal half were highly varied, so we undid the Clustal alignment for this region and present each sequence linearly, without gaps. The RGG triplets that make up the RGG boxes are shaded bold and underlined; polyglycine tracts (three or more Gs) are underlined and the C-

terminal triplets, Y/s-R/s-R, are indicated in shaded bold type. The asterisks indicate that the sequence has corresponding ESTs in the stellate ganglion database (DeGiorgis et al. 2011).

Acknowledgements: Research was supported by grants to REL from the *Fundação de Amparo à Pesquisa do Estado de Sao Paulo* (FAPESP), the *Conselho Nacional de Desenvolvimento Científico e Tecnológico* (CNPq) and the *Fundação de Apoio ao Ensino, Pesquisa e Assistência do Hospital das Clínicas da FMRP-USP* (FAEPA). JAD received financial support from the *RI-INBRE Program Grant #8 P20 GM103430-12 from the National Institute of General Medical Sciences, NIH, Bethesda, MD*. DTPL and GSL received research fellowships from FAPESP and CNPq. REL and JCR received the Productivity-in-Research fellowship from CNPq. Special thanks to Jeff Gross and Kristen Koenig, University of Texas at Austin for making available their squid embryo RNA library for data mining. Also thanks to Silvia Andrade for expert technical help. The authors declare no competing financial interests.

References

Akins MR, Berk-Rauch HE, Fallon JR (2009) Presynaptic translation: Stepping out of the postsynaptic shadow. Fronteirs in Neural Circuits 3:1-7.

Angenstein F, Evans AM, Ling S-C, Settlage RE, Ficarro S, Carrero-Martinez FA, Shabanowitz J, Hunt DF, Greenough WT (2005) Proteomic characterization of messenger ribonucleoprotein complexes bound to nontranslated or translated poly(A) mRNAs in the rat cerebral cortex. J Biol Chem 280(8):6496-6503.

Benech JC, Crispino M, Kaplan BB, Giuditta A (1999) Protein synthesis in presynaptic endings from squid brain: modulation by calcium ions. J Neurosci Res 55:776-781.

Bleher R and Martin R (2001) Ribosomes in the squid giant axon. Neurosci 107(3):527-534.

Buratti E, Brindisi A, Giombi M, Tisminetzky S, Ayala YM, Baralle FE (2005) J Biol Chem 280(45):37572-37584.

Chomczynski P and Sacchi N (1987) Single –step method of RNA acid guanidinium thiocyanate-phenol-chloroform extraction. Anal Biochem 162:156-159.

Costa MC, Mani F, Santoro W, Jr., Espreafico EM, Larson RE (1999) Brain myosin-V, a calmodulin-carrying myosin, binds to calmodulin-dependent protein kinase II and activates its kinase activity. J Biol Chem 274:15811-15819.

Court FA, Hendriks WTJ, MacGillavry HD, Alvarez J, van Minnen J (2008) Schwann cell to axon transfer of ribosomes: Toward a novel understanding of the role of glia in the nervous system. J Neurosci 28(43):11024-11029.

Crispino M, Castigli E, Capano CP, Martin R, Menichini E, Kaplan BB, Giuditta A (1993) Protein synthesis in a synaptosomal fraction from squid brain. Mol Cell Neurosci. 4:366-374.

Crispino M, Kaplan BB, Martin R, Alvarez J, Chun JT, Benech JC, Giuditta A (1997) Active polysomes are present in the large presynaptic endings of the synaptosomal fraction from squid brain. J Neurosci 17:7694–7702.

DeGiorgis JA, Cavaliere KR, Burbach JPH (2011) Identification of molecular motors in the Woods Hole squid, Loligo pealei: An expressed sequence tag approach. Cytoskeleton 68(10):566-77.

Dreyfuss G, Kim VN, Kataoka N (2002) Messenger-RNA-binding proteins and the messages they carry. Nat Rev Mol Cell Biol 3:195–205.

Eyman M, Cefaliello C, Ferrara E, De Stefano R, Lavina ZS, Crispino M, Squillace A, van Minnen J, Kaplan BB, Giuditta A (2007) Local synthesis of axonal and presynaptic RNA in squid model systems. Eur J Neurosci. 25:341-350.

Gioio AE, Lavina ZS, Jurkovicova D, Zhang H, Eyman M, Giuditta A, Kaplan BB (2004) Nerve terminals of squid photoreceptor neurons contain a heterogeneous population of mRNAs and translate a transfected reporter mRNA. Eur J Neurosci 20:865-872.

Giuditta A, Kaplan BB, van MJ, Alvarez J, Koenig E (2002) Axonal and presynaptic protein synthesis: new insights into the biology of the neuron. Trends Neurosci 25:400-404.

Haghighat N, Cohen RS, Pappas GD (1984) Fine structure of squid (Loligo pealei) optic lobe synapses. Neurosci 13(2):527-546.

He Y, Smith R (2009) Nuclear functions of heterogeneous nuclear ribonucleoproteins A/B. Cell Mol Life Sci 66:1239-1256.
Higgins DG, Sharp PM (1989) Fast and sensitive multiple sequence alignments on a microcomputer. Comput Appl Biosci 5:151–153.
Iwahashi CK, Yasui DH, An H-J, Greco CM, Tassone F, Nannen K, Babineau B, Lebrilla CB, Hagerman RJ, and Hagerman PJ (2006) Protein composition of the intranuclear inclusions of FXTAS. Brain 129:256-271.
Jimenez CR, Eyman M, Lavina ZS, Gioio A, Li KW, van der Schors RC, Geraerts WP, Giuditta A, Kaplan BB, van MJ (2002) Protein synthesis in synaptosomes: a proteomics analysis. J Neurochem 81:735-744.
Kaplan BB, Lavina ZS, Gioio AE (2004) Subcellular compartmentation of neuronal protein synthesis: new insights into the biology of the neuron. Ann N Y Acad Sci 1018:244-254.
Kim HJ, Kim NC, Wang Y-D, Scarborough EA, Moore J. etal., (2013) Mutations in prion-like domains in hnRNPA2B1 and hnRNPA1 cause multisystem proteinopathy and ALS. Nature 495:467-473.
Koenig E, Giuditta A (1999) Protein-synthesizing machinery in the axon compartment. Neurosci 89(1):5-15.
Koenig E, Martin R, Titmus M, Sotelo-Silveira JR (2002) Cryptic peripheral ribosomal domains distributed intermittently along mammalian myelinated axons. J Neurosci 20(22):8390-8400.
Kozak M (1989) The scanning model for translation: An update. J Cell Biol 108:229-241.
Krecic AM and Swanson MS (1999) hnRNP complexes: Composition, structure, and function. Curr Opin Cell Biol 11:363-371.
Lico DTP, Rosa JC, DeGiorgis JA, deVasconcelos EJR, Casaletti L, Tauhata SBF, Baqui MMA, Fukuda M, Moreira JE, Larson RE (2010) A novel 65 kDa RNA-binding protein in squid presynaptic terminals. Neurosci 166:73-83.
Maris C, Dominguez C, Allain FH (2005) The RNA recognition motif, a plastic RNA-binding platform to regulate post-transcriptional gene expression. FEBS J 272:2118–2131.
Martin KC (2004) Local protein synthesis during axon guidance and synaptic plasticity. Curr Op Neurol 14:305-310.
Martin KC, Zukin RS (2006) RNA trafficking and local protein synthesis in dendrites: An overview. J Neurosci 26(27):7131-7134.
Martin R, Vaida B, Bleher R, Crispino M, Giuditta A (1998). Protein synthesizing units in presynaptic and postsynaptic domains of squid neurons. JCell Sci 111: 3157-3166.
McLellan T (1982) Electrophoresis Buffers for Polyacrylamide Gels at Various pH. Anal Biochem 126: 94-99
Pascale A and Govoni S (2012) The complex world of post-transcriptional mechanisms: is their deregulation a common link for diseases? Focus on ELAV-like RNA-binding proteins. Cell Mol Life Sci 69:501-517.
Pekkurnaz G, Fera A, Zimmerberg-Helms J, DeGiorgis JÁ, Bezrukov L, Blank PS, Mazar J, Reese TS, Zimmerberg J (2011) Isolation and ultrastructural characterization of squid synaptic vesicles. Biol Bull 220**:**89–96.
Pfeiffer BE, Huber KM (2006) Current advances in local protein synthesis and synaptic plasticity. J Neurosci 26(27):7147-7150.
Piper M, Holt C (2004) RNA translation in axons. Annu Rev Cell Dev Biol 20:505-523.
Roberts RC, Makey D, Seal A (1966) Human transferring. Molecular weight and sedimentation properties. J Biol Chem 241(21):4907-4918.
Schuman EM, Dynes JL, Steward O (2006) Synaptic regulation of translation of dendritic mRNAs. J Neurosci 26(27):7143-7146.
Sheller RA, Tytell M, Smyers M, Bittner GD (1995) Glia-to-axon communication: enrichment of glial proteins transferred to the squid giant axon. J Neurosci Res 41(3):324-334.
Sossin WS, DesGroseillers L (2006) Intracellular trafficking of RNA in neurons. Traffic 7:1581-1589.
Sotelo-Silveira JR, Calliari A, Kun A, Koenig E, Sotelo JR (2006) RNA trafficking in axons. Traffic 7:508-515.
Sotelo JR, Canclini L, Kun A, Sotelo-Silveira JR, Calliari A, Cal K, Bresque M, DiPaolo A, Farias J, Mercer JÁ. (2014) Glia to axon RNA transfer. Develop Neurobiol 74:292-302
Steward O, Schuman EM (2003) Compartmentalized synthesis and degradation of proteins in neurons. Neuron 40:347-359.
Taylor AM, Berchtold NC, Perreau VM, Tu CH, Jeon NL, Cotman CW (2009) Axonal mRNA in uninjured and regenerating cortical mammalian axons. J Neurosci 29(15):4697-4707.

Twiss JL, Fainzilber M (2009) Ribosomes in axons – scrounging from the neighbors? Trends Cell Biol 19(5):236-243.

Vogelaar CF, Gervasi NM, Gumy LF, Story DJ, Raha-Chowdhury R, Leung K-M, Holt CE, Fawcett JW (2009) Axonal mRNAs: Characterization and role in the growth and regeneration of dorsal root ganglion axons and growth cones. Molec Cell Neurosci 42:102-115.

Wang DO, Kim SM, Zhao Y, Hwang H, Miura SK, Sossin WS, Martin KC (2009) Synapse- and stimulus-specific local translation during long-term neuronal plasticity. Science 324:1536-1540.

Willis DE, van Niekerk EA, Sasaki Y, Mesngon M, Merianda TT, Williams GG, Kendall M, Smith DS, Bassell GJ, Twiss JL (2007) Extracellular stimuli specifically regulate localized levels of individual neuronal mRNAs. J Cell Biol 178(6):965-980.

Winton MJ, Igaz LM, Wong MM, Kwong LK, Trojanowski JQ, Lee VM-Y (2008) Disturbance of nuclear and cytoplasmic TAR DNA-binding protein (TDP-43) induces disease-like redistribution, sequestration, and aggregation formation. J Biol Chem 283(19):13302-13309.

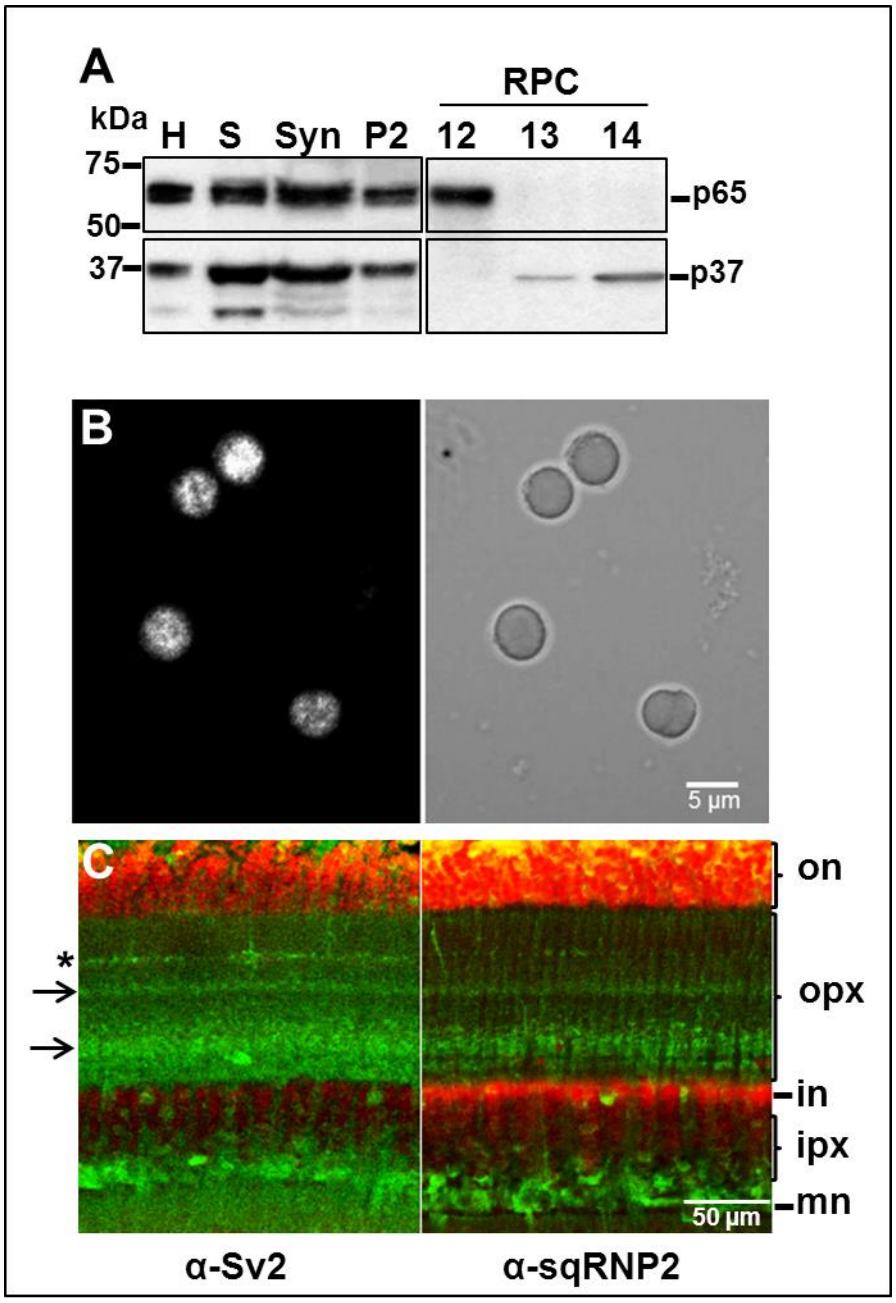
A
RPC
kDa
H
S
Syn
P2
12
13
14
75
50
37
p65
p37
B
5 µm
C
*
on
opx
in
ipx
mn
50 µm
α-Sv2
α-sqRNP2

Fig. 1

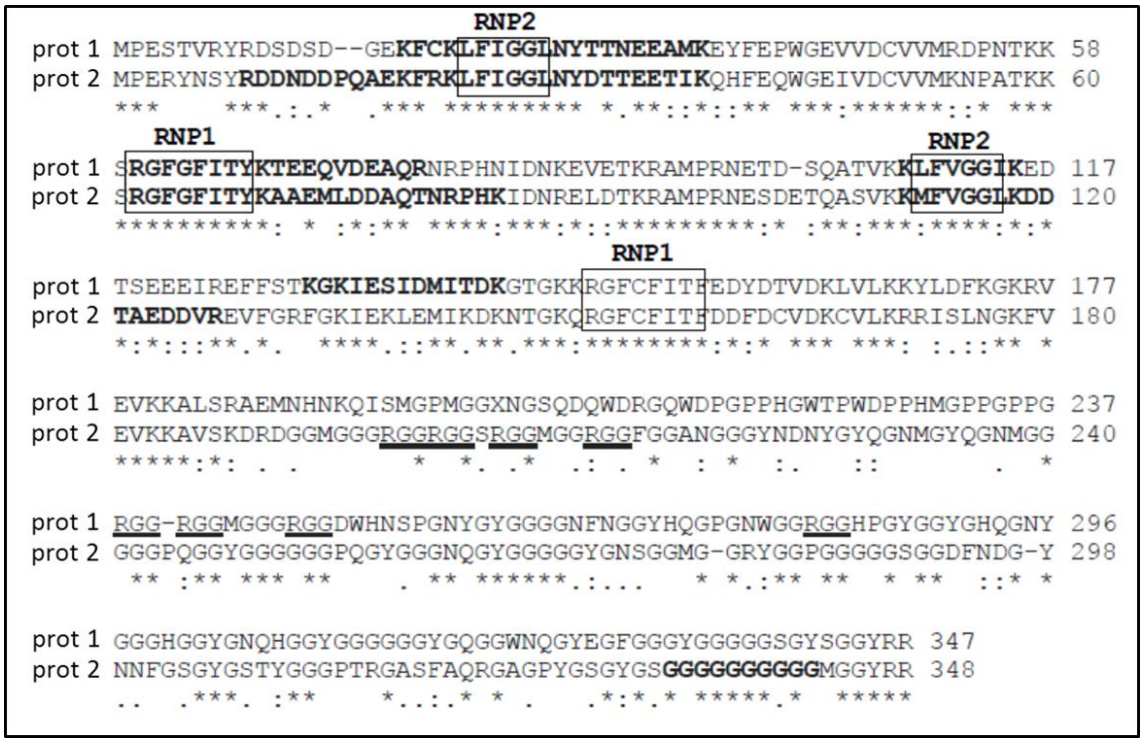

Fig. 2

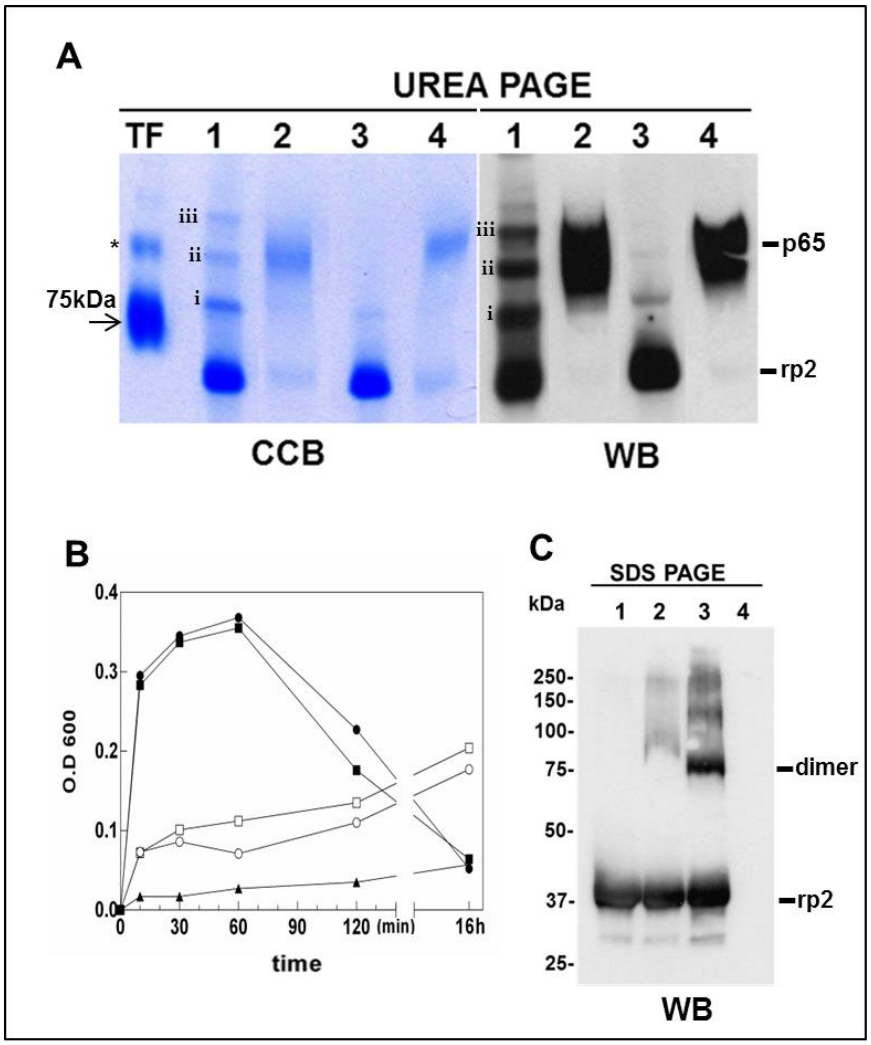
A
UREA PAGE
TF 1 2 3 4 1 2 3 4
iii
ii
i
*
75kDa
p65
rp2
CCB
WB
B
O.D 600
0.4
0.3
0.2
0.1
0.0
0 30 60 90 120 (min) 16h
time
C
SDS PAGE
kDa
1 2 3 4
250-
150-
100-
75-
50-
37-
25-
dimer
rp2
WB

Fig. 3

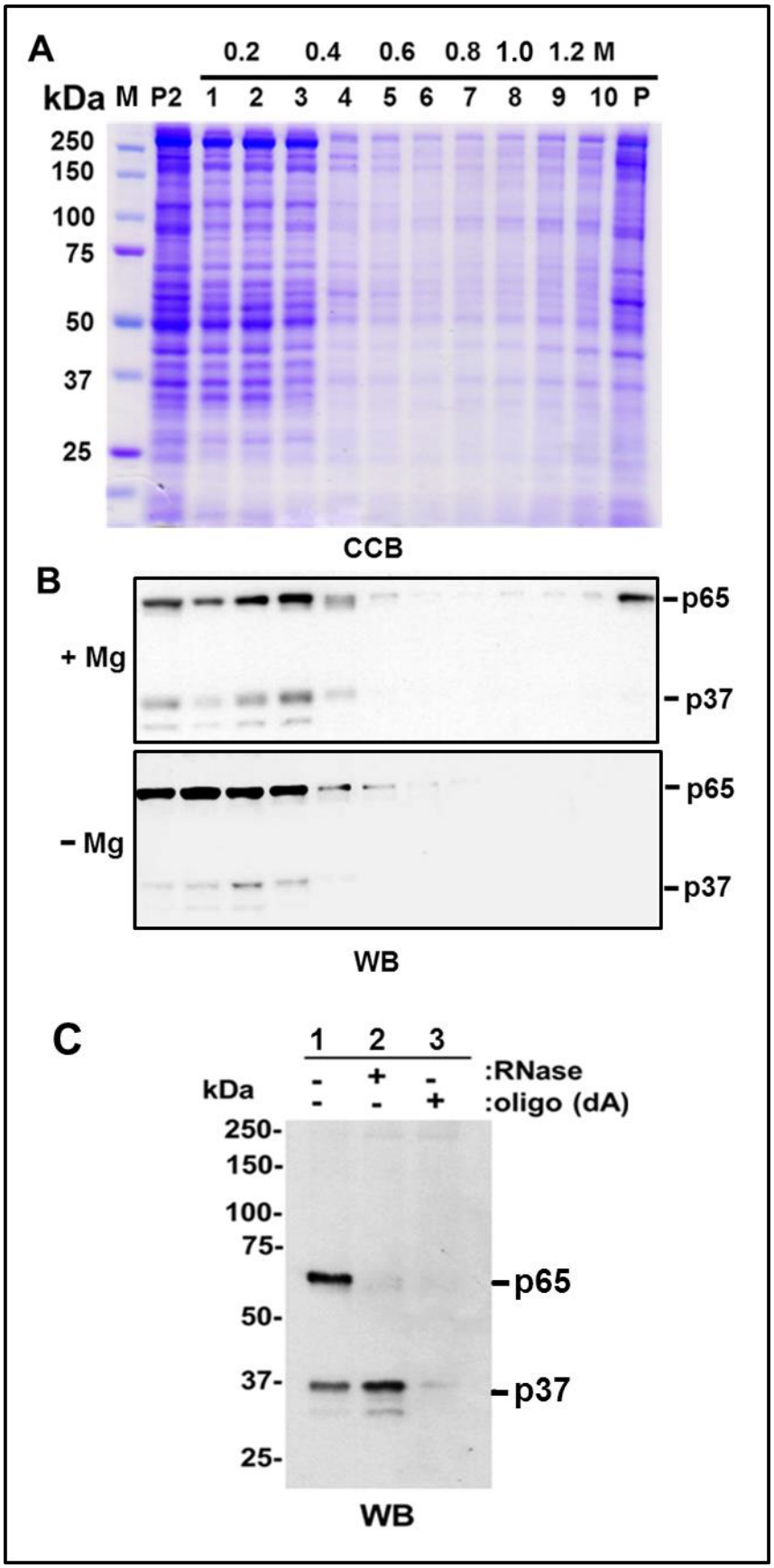
A
0.2 0.4 0.6 0.8 1.0 1.2 M
kDa M P2 1 2 3 4 5 6 7 8 9 10 P
250
150
100
75
50
37
25
CCB
B
+ Mg
p65
p37
- Mg
p65
p37
WB
C
1 2 3
kDa
- + -
- - +
:RNase
:oligo (dA)
250-
150-
100-
75-
50-
37-
25-
p65
p37
WB

Fig. 4

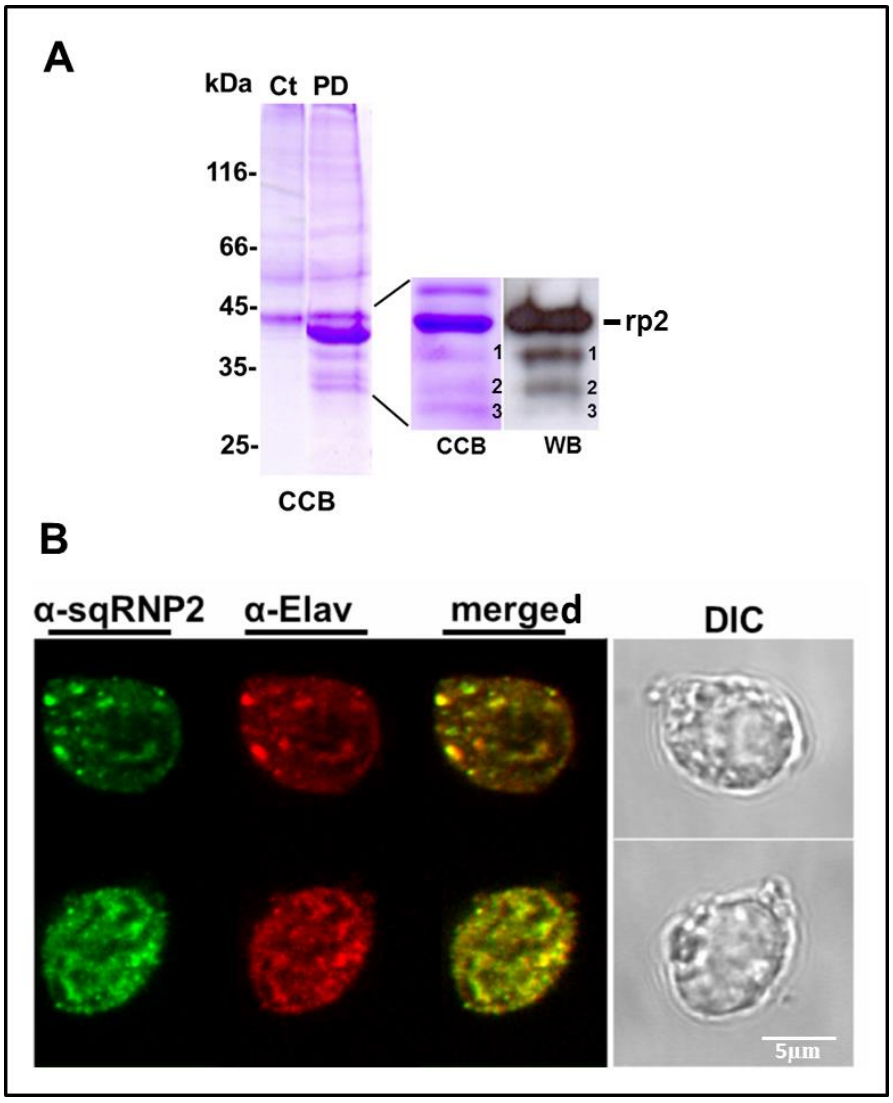
A
kDa
Ct
PD
116-
66-
45-
35-
25-
CCB
rp2
1
2
3
CCB
WB
B
α-sqRNP2
α-Elav
merged
DIC
5µm

Fig. 5


A
contig976*
isotig3766*
isotig3768*
isotig13367*
contig6207*
isotig8546*
isotig01908
isotig24490
isotig05053
isotig15030
contig976*
isotig3766*
isotig3768*
isotig13367*
contig6207*
isotig8546*
isotig01908
contig6206*
isotig24490
isotig05053
isotig15030
contig976*
isotig3766*
isotig3768*
isotig13367*
contig6207*
isotig8546*
isotig01908
contig6206*
isotig24490
isotig05053
isotig15030
contig976*
isotig3766*
isotig3768*
isotig13367*
contig6207*
isotig8546*
isotig01908
contig6206*
isotig24490
isotig05053
isotig15030
B
contig976*
isotig3766*
isotig3768*
contig6207*
isotig13367*
isotig8546*
isotig01908
contig6206*
isotig24490
isotig05053
isotig15030
contig976*
isotig3766*
isotig3768*
contig6207*
isotig13367*
isotig8546*
isotig01908
isotig05053
isotig15030
contig976*
contig6207*
isotig01908
isotig15030

Fig. 6